Available online at www.sciencedirect.com

CrossMark

ScienceDirect

Procedia Structural Integrity 19 (2019) 388–394

Fatigue Design 2019

Static and dynamic behavior of PU foams with multilayer coatings

Francesca Curà[a], Raffaella Sesana[a]*, Fabrizio Scarpa[b], Xiao-Chong Zhang[b], Hua-Xin Peng[c]

[a]DIMEAS, Politecnico di Torino, corso Duca degli Abruzzi 24, 10129 Torino, ITALY
[b] Bristol Composites Institute (ACCIS), University of Bristol, BS8 1TR Bristol, UK
c Institute for Composites Science Innovation (InCSI), School of Materials Science and Engineering, Zhejiang University, Hangzhou, 310027, PRC

Abstract

An overview on static and dynamic behavior of functional polymeric foams is presented. In particular, a PU (Poly Urethane) open cells foam was manufactured to obtain specimens with different nanostructured coatings.
An experimental campaign was performed with 7 different kind of multilayer coatings.
Quasi-static compression preconditioning and compression fatigue cycles were applied and 5 parameters were measured during cycling: Hysteresis loop area, Dissipated energy per cycle, Stiffness degradation, Secant modulus, Loss factor values.
The results show the effect of the contribution of nanoink layers to the static and cyclic behavior of foams.

Peer-review under responsibility of the Fatigue Design 2019 Organizers.

Keywords: multilayer nanocomposites; nanoinks foams; mullin effect; hyperelasticity.

1. Introduction

Polymer nanocomposite foams combine the energy absorption and lightweight properties of foams, with the added multifunctionalities of nanomaterials dispersed within their structure, with enhanced strength (Dolomanova et al. (2011), Chen et al. (2014), Chen et al. (2011)) and dielectric properties (Chen et al. (2014), Athanasopoulos et al. (2012), Dai et al. (2012)), sound and vibration damping (Verdejo et al. 2009), Lee et al. (2012), Sung et al. (2007), Bandarian et al. (2011)), energy dissipation under compressive loading (Bezazi and Scarpa (2007)). This damping capacity is due to the energy dissipation mechanisms involved in the polymer/carbon nanotube (CNT) interface that is: nanotube/nanotube interfacial sliding and – in the case of multi-walled carbon nanotubes (MWCNTs) – the coaxial

2452-3216 © 2019 The Authors. Published by Elsevier B.V.
Peer-review under responsibility of the Fatigue Design 2019 Organizers.
10.1016/j.prostr.2019.12.042

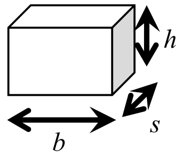

Fig. 1. specimen designation and main dimensions.

The following parameters were calculated by means of processing resulting data, for different number of cycles: the area of the hysteresis cycle, the dissipated energy per cycle, the secant modulus of the cycle, the stiffness degradation (rigidity loss) and the loss factor.

The hysteresis cycle area was calculated by means of numerical integration by means of the trapezium rule (Davis and Rabinowitz (2007)) on the stress-strain diagram as already done in Curà and Sesana (2014).

The dissipated energy is assumed to be related to the hysteresis cycle area (Lazan (1968)) for elastic materials; then it was obtained as the area of the hysteresis cycles times the specimen volume.

The secant modulus was calculated as the ratio between the difference of maximum and minimum stress and the difference between the corresponding maximum and minimum strain of the cycle for hysteresis cycles with elliptical shape.

The stiffness degradation *SD* was calculated as the ratio between the maximum stress in a cycle and the maximum stress that of the first cycle.

The loss factor η was calculated as the ratio between *D*, the energy dissipated per cycle (or the energy that must be supplied to the system to maintain steady state conditions) and *W*, the total (kinetic plus potential) energy associated with the vibration time 2π (Ungar and Kerwin (1962)):

$$\eta = \frac{D}{2\pi W}$$

3. Results and discussion

The results of quasi-static cyclic preconditioning of specimens are reported in Figure 2 and 3. In Figure 2 the 5 preconditioning cycles are reported for pure material PU, for 4PU and 4MW specimens as an example. The change in slope between the two linear trends occurs for strain values about 5%. Increasing the number of coating layers increases the maximum stress and the area of the hysteresis cycle.

Figure 3 shows the average decrement $\Delta\sigma_{max}$ of the maximum stress σ_{max} on five specimens per material from the first to the fifth cycle in quasi-static cycling (Figure 3*a*). The same value, normalized with respect to the maximum stress in the first cycle and in % value, $\%\Delta\sigma_{norm}$, is also reported (Figure 3*b*). It can be observed that this decrement of maximum stress (stress softening) corresponds to the hyperelastic behavior described by Mullin effect (Govindjee and Simo (1991), Ogden and Roxburg (1999)).

This means that damage phenomena are taking place during uniaxial static compression. The contribution to damage may be split in two parts, the first part can be accounted to pure foam (PU) and it is constant for all specimens; the second one can be attributed to coating layers damage (Bandarian et al (2011), Zhang et al (2016), Zhang et al (2016)).

This second contribution is quantitatively different for different specimens as demonstrated from the analysis of Figure 3. Similar results can be found in cyclic experiments.

(a) *(b)* *(c)*

Figure 2: average hysteresis cycles for PU (a) specimen, 4PU (b) and 4MW (c) specimens in quasi-static cycling

(a) *(b)*

Figure 3: average decrement in maximum stress in absolute value *(a)* and % normalized (b) in quasi-static cycling

From the analysis of Figure 3 it can be observed that the presence of different coating layers strongly influences the foams behavior, providing in all cases a stiffening effect. This behavior changes substantially during the quasi-static cyclic preconditioning; in particular, PU layers show a linear decrement in maximum stress by increasing the number of layers, while MW layers show a higher degradation that appears to not be influenced by the layers number increasing.

In the following Tables 1-3 the results of the experimental cyclic tests are reported. In particular in Table 1 the stiffness degradation, in Table 2 the secant modulus, in Table 3 the loss factor. The area of the hysteresis cycle and the dissipated energy per cycle were used to calculate the loss factor values.

Table 1. Stiffness degradation [-].

	PU	1PU	4PU	1MW	2MW	3MW	4MW
1% 1 Hz	0,078	0,116	0,322	0,256	0,237	0,228	0,101
1% 10 Hz	0,196	0,225	0,252	0,207	0,207	0,232	0,212
0,5% 1 Hz	0,237	0,349	0,328	0,323	0,374	0,075	0,119
0,5 % 10 Hz	0,169	0,268	0,288	0,230	0,264	0,293	0,194

Table 2. Secant modulus [kPa].

	PU	1PU	4PU	1MW	2MW	3MW	4MW
1% 1 Hz	15034,3	30483,3	12614,9	3661,7	3537,0	3466,2	19492,0
1% 10 Hz	10155,9	4554,2	15507,4	40279,0	2431,9	15695,7	98802,5
0,5% 1 Hz	18653,7	22124,5	53449,1	27728,4	18286,3	47237,8	13994,6
0,5 % 10 Hz	5626,6	3885,9	4329,0	13818,7	15626,1	24211,9	1842,3

Table 3. Loss factor [-].

	PU	1PU	4PU	1MW	2MW	3MW	4MW
1% 1 Hz	0,257	0,078	0,058	0,247	0,187	0,183	0,271
1% 10 Hz	0,011	0,023	0,012	0,167	0,085	0,086	0,355
0,5% 1 Hz	0,017	0,009	0,001	0,007	0,004	0,036	0,103
0,5 % 10 Hz	0,015	0,003	0,010	0,004	0,003	0,006	0,002

In Figure 4 and 5, as an example, the values of stiffness degradation to evaluate the effect of the PU and CNT coatings in different strain and frequency conditions are reported. In Figure 6 and 7 analogous results are shown for Loss factor.

SD [-]

SD [-]

SD [-]

SD [-]

Fig. 4. Stiffness degradation in different strain and frequency conditions for different number of PU coating layers.

SD [-]

SD [-]

SD [-]

SD [-]

SD [-]

Fig. 5. Stiffness degradation in different strain and frequency conditions for different number of CNT coating layers.

Fig. 6. Loss factor in different strain and frequency conditions for different number of PU coating layers.

Fig. 7. Loss factor in different strain and frequency conditions for different number of CNT coating layers.

From the analysis of Figures 4-7 it can be observed that the test frequency influences the foams characteristics.

For 10 Hz and higher strain, differences in stiffness degradation (see Figures 4 and 5) between coated and uncoated specimens become lower, regardless the kind of coating, PU or CNT.

In Figures 6 and 7 higher loss factor values can be observed for higher strains. The influence of the test frequency doesn't appear in these first results.

For this kind of foams, a plateau is usually reached for 5% strain and then the loss factor tends to decrement for high strains. In this case of lower % values of strain, probably other effects are presents in the case of coated foams, to affect the behavior of loss factor.

4. Conclusions

In the present paper the results of an experimental activity on multilayer nanocoated PU open cell foams are presented. Quasi-static and cyclic compression tests were performed. The particular aim was to characterize the effect of different number and kind of layers: PU and CNT nanoinks.

The results of quasi-static cyclic preconditioning of specimens show that an increasing number of coating layers increases the maximum stress and the area of the hysteresis cycle.

It can also be observed for all specimens a decrement in the maximum stress with cycles (stress softening) and this phenomenon is more evident increasing the number of layers. This difference in damaging behavior can be attributed to the coating layer contribution. This trend is linear for PU layers and non-linear for MW layers.

For cyclic characterization the following parameters, obtained from the hysteresis loops, were chosen: Stiffness degradation, Secant modulus and Loss factor.

From this first analysis, it appears that both strain amplitude and test frequency influence the foams characteristics.

Further tests will validate from a quantitative point of view these evidences.

References

Athanasopoulos, N., A. Baltopoulos, A., M. Matzakou, M., Vavouliotis, A., Kostopoulos, V., 2012. Electrical conductivity of polyurethane/MWCNT nanocomposite foams. Polym Composite 33(8), 1302-1312.

Bandarian, M., Shojaei, A., Rashidi, A.M., 2011. Thermal, mechanical and acoustic damping properties of flexible open-cell polyurethane/multi-walled carbon nanotube foams: effect of surface functionality of nanotubes. Polym Int, 60(3), 475-482.

Bezazi, A., Scarpa, F., 2007. Mechanical behaviour of conventional and negative Poisson's ratio thermoplastic polyurethane foams under compressive cyclic loading. International Journal of fatigue 29, 922-930.

Chen, L.M., Schadler, L.S., Ozisik, R., 2011. An experimental and theoretical investigation of the compressive properties of multi-walled carbon nanotube/poly(methyl methacrylate) nanocomposite foams. Polymer, 52(13), 2899-2909.

Chen, M.T., Zhang, L., Duan, S.S., Jing, S.L., Jiang, H., Luo, M.F., Li, C.Z.2014. Highly conductive and flexible polymer composites with improved mechanical and electromagnetic interference shielding performances. Nanoscale 6(7), 3796-3803.

Chen, Y.J., Li, Y., Chu, B.T.T., Kuo, I.T., Yip, M., Tai, N., 2015. Porous composites coated with hybrid nano carbon materials perform excellent electromagnetic interference shielding. Composites: Part B , 70, 231-237.

Curà, F., Sesana, R., 2014. Mechanical and thermal parameters for high-cycle fatigue characterization in commercial steels. Fatigue Fract Engng Mater Struct 37, 883–896.

Dai, K., Ji, X., Xiang, Z.D., Zhang, W.Q., Tang, J.H., Li, Z.M., 2012. Electrical Properties of an Ultralight Conductive Carbon Nanotube/Polymer Composite Foam Upon Compression. Polym-Plast Technol, 51(3), 304-306.

Davis, P. J., Rabinowitz, P., 2007. Methods of Numerical Integration Dover Books on Mathematics Series. Dover Publications, Inc, Mineola, N.Y.

Dolomanova, V., Rauhe, J.C.M., Jensen, L.R., Pyrz, R., Timmons, A.B. 2011. Mechanical properties and morphology of nano-reinforced rigid PU foam. Journal of Cellular Plastics. J Cell Plast 47(1), 81-93.

Govindjee, S., Simo, S., 1991. A micro-mechanically based continuum damage model for carbon black-filled rubbers incorporating Mullins' effect, J. Mech. Phys. Solids 39(I), 87-112.

Hu, Z.L., Pang, Q., Ji, G.Q., Wu, G.H., 2018. Mechanical behaviors and energy absorption properties of Y/Cr and Ce/Cr coated open-cell nickel-based alloy foams. Rare Met. 37(8), 650-661.

Kang, T., Yoon, J., Kim, D., Kum, S., Huh, Y., Hahn, J., Moon, S., Lee, H., Kim, Y., 2007. Sandwich-Type Laminated Nanocomposites Developedby Selective Dip-Coating of Carbon Nanotubes. Adv. Mater 19, 427-432.

Lazan, B. J., 1968. Damping of materials and members in structural mechanics (Oxford Pergamon Press Oxford).

Lee, J., Kim, G.H., Ha, C.S., 2012. Sound Absorption Properties of Polyurethane/Nano-Silica Nanocomposite Foams. J Appl Polym Sci, 123(4), 2384-2390.

Ogden, R.W., Roxburgh, D.G. 1999. A pseudo–elastic model for the Mullins effect in filled rubberProceedings of the Royal Society of London. 455, 2861–2877.

Sung, C.H., Lee, K.S., Lee, K.S., Oh, S.M., Kim, J.H., Kim, M.S., Jeong, R.M., 2007. Sound damping of a polyurethane foam nanocomposite. Macromol Res, 15(5), 443-448.

Verdejo, R., Stämpfli, R., Alvarez-Lainez, M., Mourad, S., Rodriguez-Perez, M.A., Brühwiler, P.A., Shaffer, M., 2009. Enhanced acoustic damping in flexible polyurethane foams filled with carbon nanotubes. Compos Sci Technol, 69(10), 1564-1569.

Ungar, E.E., Kerwin, E.M. 1962. Loss factors of viscoelastic systems in terms of energy concepts. The Journal of the Acoustical Society of America, 34(7), 954-957.

Zhang, X.C., Peng, H.X., Limmack, A.P., Scarpa, F., 2014. Viscoelastic damping behaviour of cup stacked carbon nanotube modified epoxy nanocomposites with tailored interfacial condition and re-agglomeration. Compos Sci Technol, 105, 66-72.

Zhang, X.C., Scarpa, F., McHale, R., Limmack, A.P., Peng, H.X., 2016. Carbon nano-ink coated open cell polyurethane foam with micro-architectured multilayer skeleton for damping applications. RSC Advances, 6(83), 80334-80341.